Expanded View Figures

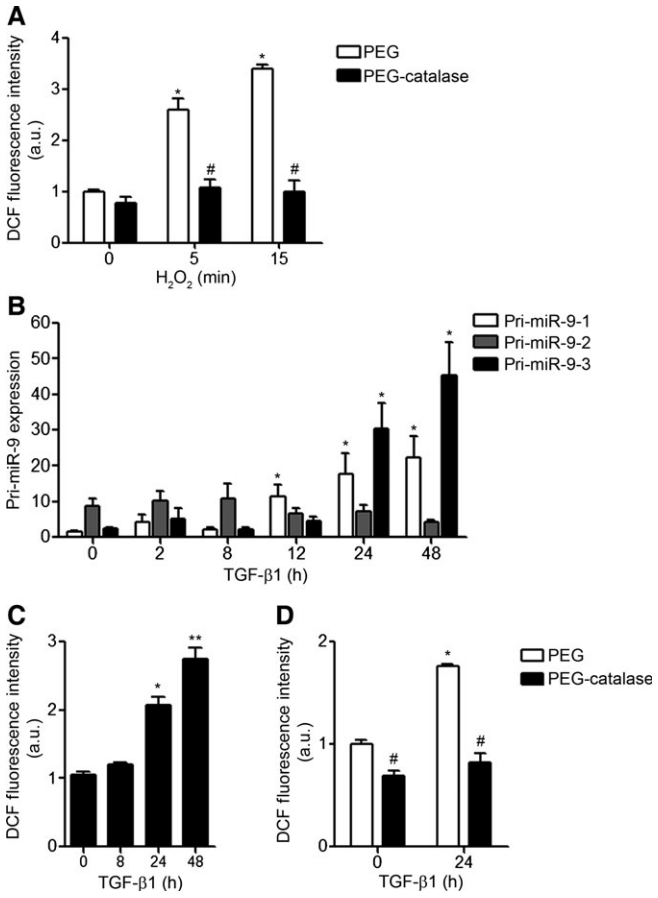

Figure EV1. Effect of PEG-catalase on H_2O_2- and TGF-β1-induced ROS production and effect of TGF-β1 on the expression of miR-9-5p precursors and on ROS production in HFL-1 cells.

A Lung fibroblasts were treated with 100 μM H_2O_2 for the indicated times after pre-incubation for 2 h either with polyethylene glycol (PEG) or with 100 U/ml PEG-catalase (n = 3–5). Intracellular ROS production was measured using 2′,7′-dichlorofluorescein diacetate (DCFH-DA) reagent and analyzed by FACS.

B qRT–PCR analysis of miR-9-5p primary transcripts (pri-miR-9) levels in HFL-1 cells stimulated with 5 ng/ml TGF-β1 for the indicated times (n = 4–7).

C Intracellular ROS production in HFL-1 cells treated with 5 ng/ml TGF-β1 for the indicated times was measured as described in (A) (n = 3–5).

D Intracellular production of ROS in HFL-1 cells pre-treated as described above and treated with 5 ng/ml TGF-β1 for 24 h was measured as described in (A) (n = 3–5).

Data information: Bar graphs show mean ± SEM; two-tailed Mann–Whitney U-test and Kruskal–Wallis non-parametric ANOVA (B); $^{*}P < 0.05$, $^{**}P < 0.01$ compared to control cells and $^{\#}P < 0.05$ compared to control cells at the same time point. a.u., arbitrary units.

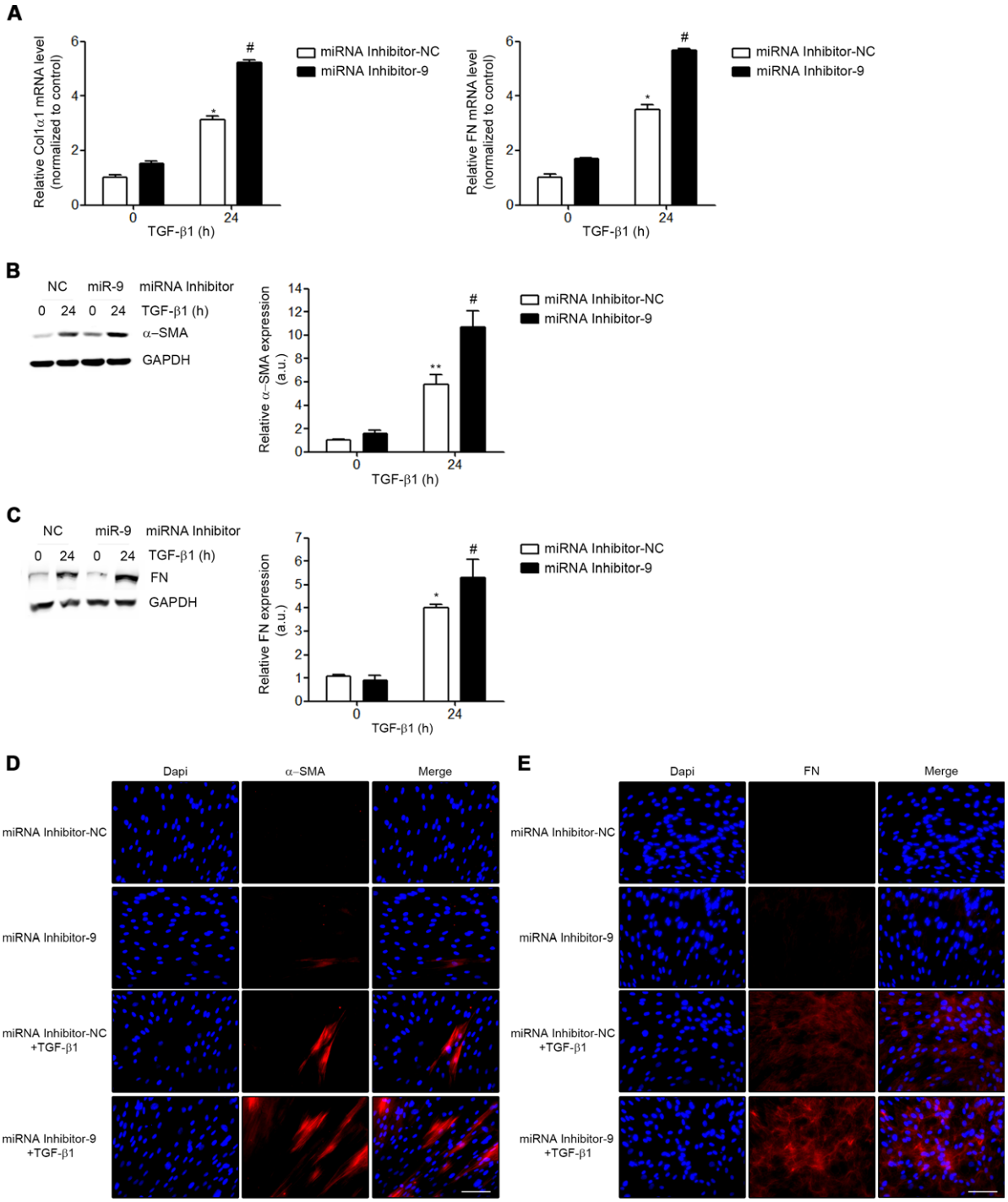

Figure EV2. Inhibition of miR-9-5p amplifies TGF-β1-induced transformation of human lung fibroblasts into myofibroblasts.

A qRT–PCR analysis of Col1α and FN (n = 4) expression levels in HFL-1 cells transfected with 40 nM miRNA inhibitor NC (control) or miRNA inhibitor-9-5p and treated with 5 ng/ml TGF-β1 for 24 h.

B, C Protein levels (left) of α-SMA (n = 5) (B) and FN (n = 4) (C) in HFL-1 cells described in (A). Quantification of protein expression (right). a.u., arbitrary units.

D, E Fluorescence microscopy images of HFL-1 cells stained with specific antibodies against α-SMA (D, middle panels) and FN (E, middle panels) after transfection as described in (A) and TGF-β1 treatment for 24 h (n = 3). Nuclei were stained with DAPI (blue). Scale bars: 100 μm.

Data information: All bar graphs show mean ± SEM; two-tailed Mann–Whitney U-test; $^{*}P < 0.05$, $^{**}P < 0.01$ compared to control cells and $^{\#}P < 0.05$ compared to its corresponding negative control time point.

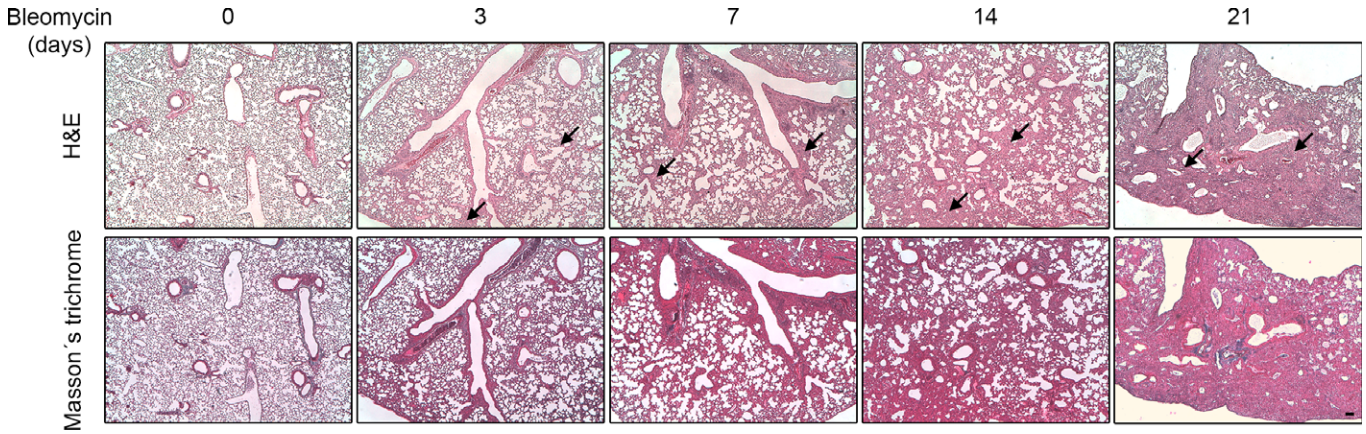

Figure EV3. Histopathological changes of lung tissue in mice treated with bleomycin.
Microphotographs of H&E (upper panels) and Masson's trichrome (bottom panels) staining of lung tissue sections from saline-treated control (day 0) as well as from orotracheally bleomycin-treated mice (1.5 U/kg body weight in 40 μl saline serum) for the indicated times (n = 3 mice per group). H&E showed intact alveoli and normal interstitium in lungs of control mice and gradually increased areas of alveolar and interstitial fibrosis (black arrows), lung alveoli destruction and interstitium thickening in lungs of bleomycin-treated mice. Intense blue Masson's staining indicates regions with collagen deposition. Scale bar: 100 μm.

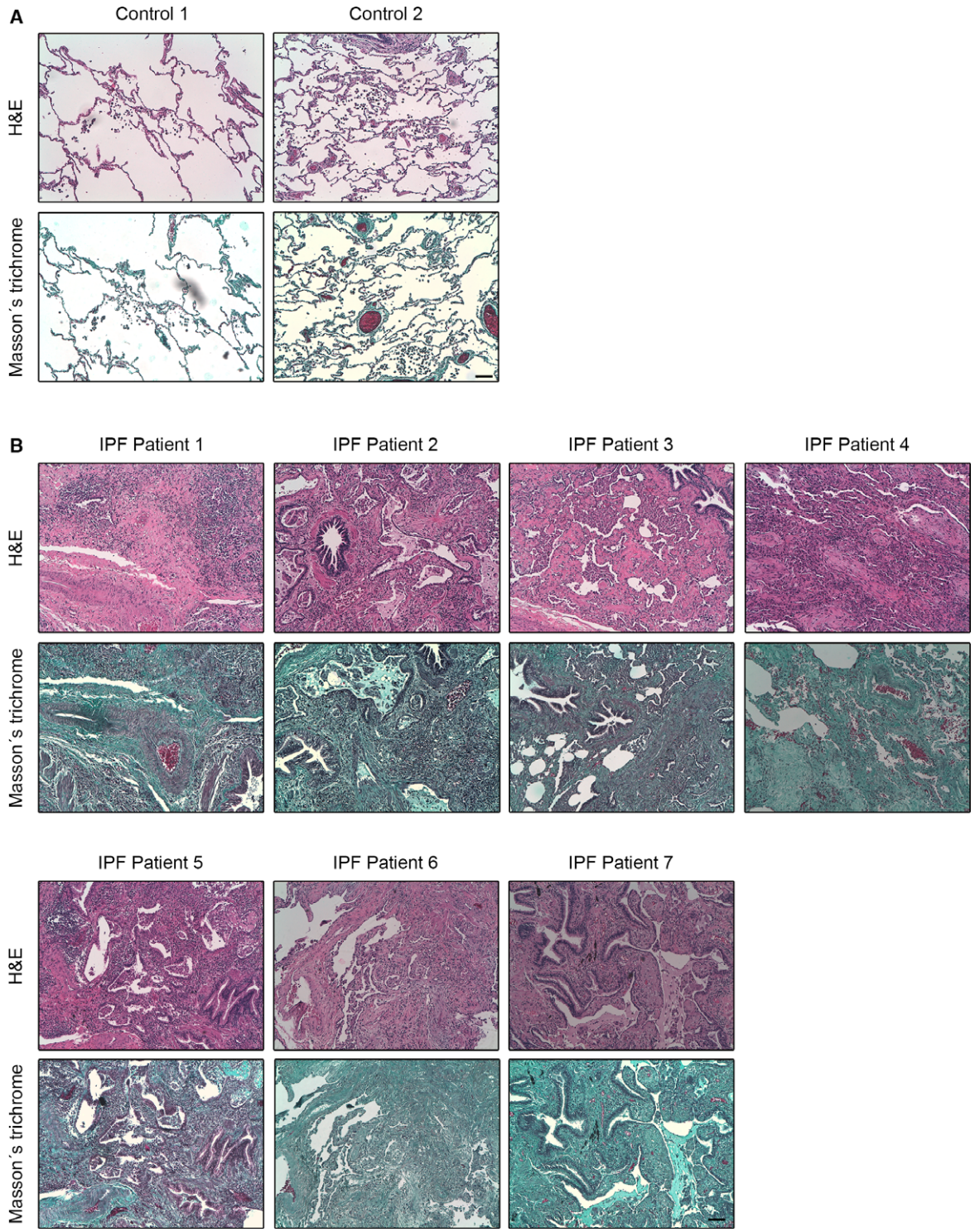

Figure EV4. Histological characterization of human lung tissue of IPF patients.

A, B Microphotographs of H&E (upper panel in each case) and Masson's trichrome (bottom panel in each case) staining in paraffin-embedded lung tissue sections from two histologically normal lungs (controls) (A) and seven IPF patients (B). As it can be observed in (A) control lung tissue is characterized by a thin pulmonary alveolar epithelium. Neither fibroblast nor ECM deposits are present in the interstitium. In IPF patients (B), an extensive pulmonary fibrosis was observed in all the specimens analyzed. Alveolar interstitium is fully occupied by fibroblasts, inflammatory infiltrates and markedly visible ECM deposits (blue in Masson's staining for collagen). Alveolar epithelium is barely observed due to fibrosis development. All images are shown at equal magnification. Scale bar: 100 μm.

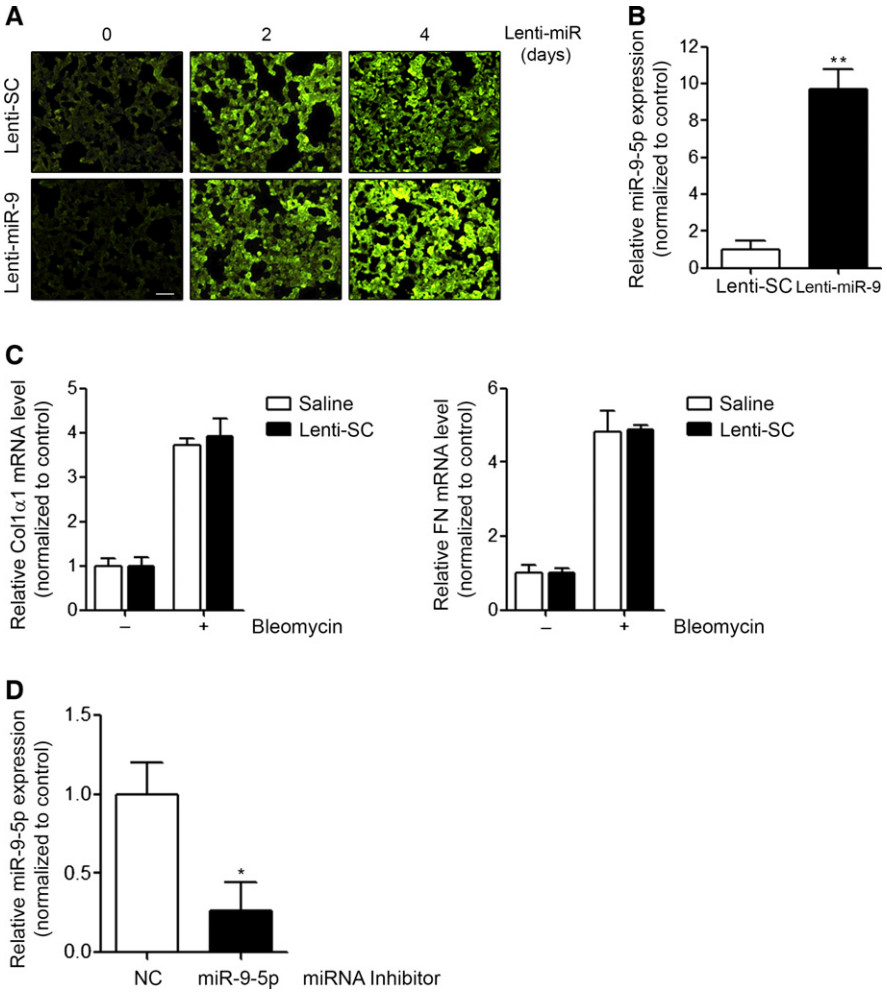

Figure EV5. Determination of miR-9-5p delivery and quantification of miR-9-5p expression level after lentiviral vector infection.

A GFP-expressing fluorescence images of frozen lung sections from mice orotracheally instilled with lenti-SC (control) or lenti-miR-9 vector (1×10^6 i.f.u./mouse) for the indicated days (n = 3 mice in each group). Scale bar: 100 μm.

B qRT–PCR analysis of miR-9-5p expression in lungs from mice after 4 days of lentiviral infection (n = 6 mice per group).

C qRT–PCR analysis of Col1α1 and FN in lungs from mice administered saline or lenti-SC 4 days before orotracheal bleomycin instillation (1.5 U/kg body weight in 40 μl saline serum) and sacrificed 14 days after treatment (n = 3 mice per group).

D qRT–PCR analysis of miR-9-5p expression in lungs from mice administered miRNA inhibitor NC (control) or miRNA inhibitor-9-5p (7 mg/kg body weight in 40 μl saline). The miRNA inhibitor was instilled at days −4 and −2 before sacrifice (n = 4 mice per group).

Data information: All bar graphs show mean ± SEM; two-tailed Mann–Whitney U-test; *$P < 0.05$, **$P < 0.01$ compared to its corresponding negative control condition; no significant differences between saline and lenti-SC-treated mice were found.